DOI: 10.1002/chem.201001179

Spin Crossover versus Low-Spin Behaviour Exhibited in 2D and 3D Supramolecular Isomers of $[Fe^{II}(2,4\text{-bpt})_2]\cdot$Guest**

Xin Bao,[a] Jun-Liang Liu,[a] Ji-Dong Leng,[a] Zhuojia Lin,[a] Ming-Liang Tong,*[a] Masayuki Nihei,[b] and Hiroki Oshio[b]

The bistable properties (magnetic, structure and colour) of spin crossover (SCO) materials have resulted in a bright future for their applications as molecular memory, molecular switches, molecular sensors, data storage and display devices.[1] Spin transitions (STs) between high- (HS) and low-spin (LS) states can be achieved by external stimuli, such as temperature, pressure, light, magnetic or electrical switching.[2] From practical aspects, the design and the synthesis of SCO compounds with high transition temperatures, wide thermal hysteresis and thermochroism are of crucial importance. Two strategies have been universally acknowledged to improve the cooperatives: 1) to construct covalently bridged coordination polymers; 2) to enrich intermolecular interactions, such as hydrogen bonding and π–π stacking.[3] However, in reality, it is hard to predict theoretically the SCO property of a material until it has been characterised. The sensitivity of the SCO property to subtle changes[4–5] does cause problems, but from another perspective, it may also be viewed as an opportunity to deepen our knowledge of the nature of SCO. To this end, the rich structural diversity of supramolecular isomers provided us a useful and unique perspective to understand structure–property relationships. As a branch of isomerism, polymorphism-dependent SCO compounds are not uncommon,[6] however, most of which are mononuclear. To the best of our knowledge, only two examples focus on structural isomerism and another shows catenane isomerism-dependent SCO properties.[7]

Herein, we report the crystal structures and physical properties of four supramolecular isomers based on $[Fe(2,4\text{-bpt})_2]\cdot$guest (2,4-Hbpt = 3-(2-pyridyl)-5-(4-pyridyl)-1,2,4-triazole): a 2D SCO polymer $[Fe(2,4\text{-bpt})_2]$ (**1**·Fe), two LS twofold interpenetrated 3D coordination polymers with NbO topology, $[Fe(2,4\text{-bpt})_2]\cdot 2.17\,H_2O$ (**2a**) and $[Fe(2,4\text{-bpt})_2]\cdot 2.5\,H_2O$ (**2b**) and a LS non-interpenetrated 3D coordination polymer with NbO topology, $[Fe(2,4\text{-bpt})_2]\cdot 4$ dioxane$\cdot 4\,H_2O$ (**3**). It should be mentioned that these complexes include all kinds of isomers except for optical isomers, that is, structural, conformational and catenane supramolecular isomerism.[8] Moreover, a cobalt analogue and a Fe−Co solid solution species: $[Co(2,4\text{-bpt})_2]\cdot 0.5\,H_2O$ (**1**·Co) and $[Fe_xCo_{1-x}(2,4\text{-bpt})_2]$ ($x = 0.93$) (**1**·Fe–Co) have also been synthesised and characterised. The latter compound allows us to investigate SCO properties in a doped system. Our work provides a good example to study magneto–structural relationships.

We choose the 2,4-Hbpt ligand mainly for the following reasons: 1) as a variant of the well-studied ligand 2,2-Rbpt (2,2-Rbpt = 4-substituted 3,5-di(2-pyridyl)-1,2,4-triazole), it should also provide an appropriate ligand field favouring the occurrence of SCO;[9] 2) it is a good candidate to construct a coordination polymer by using the 4-position N atom, thus enhancing cooperation between SCO sites; 3) the ligand can take on abundant conformations due to its rotatable feature, thus resulting in a variety of isomers and fits our need to study structure-dependent SCO properties.

All products are synthesised in solvothermal conditions at 160 °C for 3 days. However, different solvent media have an important influence on the final products. By hydrothermal treatment, five products are captured, namely, two mononuclear polymorphs based on $[Fe(2,4\text{-bpt})_2(H_2O)_2]$,[10] **1**·Fe, **2a** and **2b**. However, there are problems with low yields for all products and also poor reproducibility. So it was laborious work to collect pure **1**·Fe to study its magnetic behaviour.

[a] X. Bao, J.-L. Liu, J.-D. Leng, Dr. Z. Lin, Prof. Dr. M.-L. Tong
Key Laboratory of Bioinorganic
and Synthetic Chemistry of Ministry of Education
State Key Laboratory of Optoelectronic Materials and Technologies
School of Chemistry & Chemical Engineering
Sun Yat-Sen University
Guangzhou 510275 (P.R.China)
Fax: (+86) 20-8411-2245
E-mail: tongml@mail.sysu.edu.cn

[b] Dr. M. Nihei, Prof. Dr. H. Oshio
Graduate School of Pure and Applied Sciences
University of Tsukuba, Tennodai 1-1-1, Tsukuba 305-8571 (Japan)

[**] 2,4-Hbpt = 3-(2-pyridyl)-5-(4-pyridyl)-1,2,4-triazole

Supporting information for this article is available on the WWW under http://dx.doi.org/10.1002/chem.201001179.

With the inspiration of high yields of a single product of **1**·Co by changing ferrous salt for a cobalt salt, a seed-induced synthetic method[6e,11] came to mind and has been proven successful. Adding a small amount of cobalt salt to an aqueous solution of $FeCl_2 \cdot 4H_2O$, 2,4-Hbpt and KNCS gave large crystals of **1**·Fe–Co in 44% yield. Compound **2a** crystallised as a pure product in 60% yield by treatment with methanol. The non-interpenetrated isomer **3** was stabilised by the use of larger solvated dioxane molecules as a template, and also appeared as a single-phase product but in low yield.

The studies of molar susceptibilities of **1**·Fe and **1**·Fe–Co denote abrupt SCO with thermal hystereses. Plots of $\chi_M T$ versus T for polycrystalline samples of these compounds are shown in Figure 1. For **1**·Fe, upon cooling, the $\chi_M T$ value

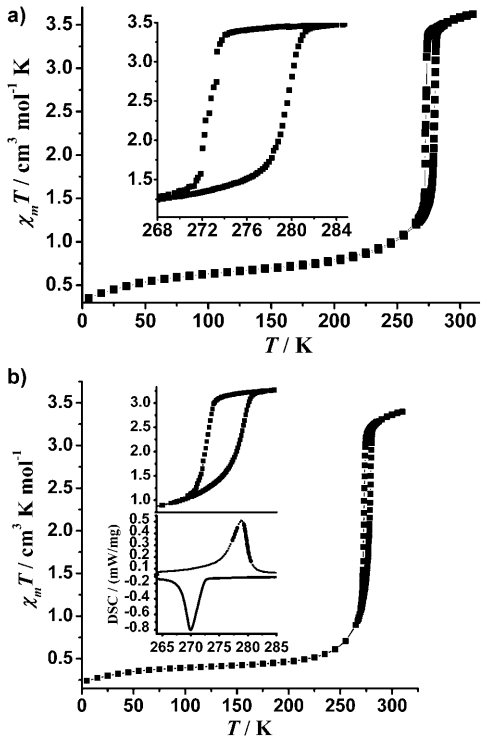

Figure 1. $\chi_m T$ versus T curves for **1**·Fe (a) and **1**·Fe–Co (b) upon heating and cooling. Insets: Expansion of the magnetic data in the hysteresis range for **1**·Fe (a) and **1**·Fe–Co and DSC curve (b).

drops slowly from 3.6 to 3.4 $cm^3 K mol^{-1}$ between 310 and 275 K, then drops sharply to 1.35 $cm^3 K mol^{-1}$ at 270 K, which indicates an abrupt ST with $T_{1/2\downarrow} = 273.4$ K. Below 275 K, the $\chi_M T$ value continuously decreases to reach 0.35 $cm^3 K mol^{-1}$ value at 5 K. Further continued measurements in the warming mode, compound **1**·Fe displays a quasi-parallelogram hysteresis of 6.8 K with $T_{1/2\uparrow} = 278.8$ K. The Co^{II}-doped sample, **1**·Fe–Co, displays a triangular hysteresis of 5.3 K wide ($T_{1/2\downarrow} = 272.2$ K, $T_{1/2\uparrow} = 277.5$ K). The comparison of two samples indicates noticeable changes in their SCO behaviour, namely, more gradual ST in the warming mode and subsequently a narrower hysteresis loop for **1**·Fe–Co. These phenomena correspond with metal dilution effect.[12]

A Mössbauer spectrum of **1**·Fe–Co measured at 20 K showed a doublet with parameters of $\delta = 0.50$ and $\Delta E_Q = 1.09$ mms^{-1}, indicating that the Fe^{II} ion is in the LS state (Figure S8 in the Supporting Information).

A differential scanning calorimetry (DSC) scan of **1**·Fe–Co was essentially in accordance with the magnetic measurement (Figure 1b, inset). The transition temperatures obtained from DSC in the cooling and warming mode are 270.0 and 278.8 K, respectively, thus defining a 8.8 K wide hysteresis. The corresponding thermodynamic parameters are $\Delta H = 11.8$ $kJ mol^{-1}$ and $\Delta S = 42.4$ $J K^{-1} mol^{-1}$ in the warming mode and $\Delta H = -11.6$ $kJ mol^{-1}$ and $\Delta S = -43.0$ $J K^{-1} mol^{-1}$

The crystal structures of the six complexes have been solved at various temperatures to detect their spin states. For the four Fe^{II} isomers, despite different structural architectures, their frameworks are all constructed of similar [Fe(2,4-bpt)$_4$] building blocks, except for some subtle differences. The Fe^{II} ion lies at the centre of a distorted [FeN_6] coordination unit. Four equatorial sites are occupied by two chelating 2,4-bpt ligands in a *trans* configuration, while the axial positions are occupied by the 4-position N atoms of two 2,4-bpt ligands (Scheme 1). The major difference in the building

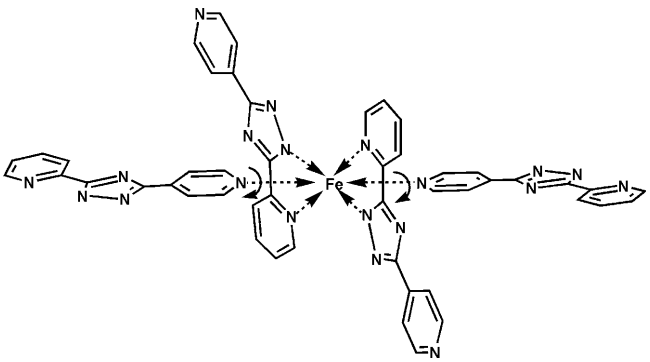

Scheme 1. Schematic representation of the [Fe(2,4-bpt)$_4$] building block.

blocks of the four isomers is the relative orientation of the axial and the equatorial ligands. A rotation of the axial ligands will not change the octahedral environment of the Fe^{II} ion, but will result in different directions of the Fe···Fe connections, thus playing a key role in the formation of different frameworks, especially the dimensionality. In addition, the different extents of deviation from a co-planar conformation of the ligand also play a subtle role in the formation of different isomers.

1·Fe, **1**·Co and **1**·Fe–Co are isostructural to a previously reported complex, [Mn(2,4-bpt)$_2$].[13] They adopt monoclinic $P2_1/n$ space groups at all temperatures. Through the diagnostic of average M–N bond lengths (<M–N>) (Table S1 in the Supporting Information), the metal centre in **1**·Co are in the HS state, whereas in **1**·Fe and **1**·Fe–Co, Fe^{II} ions experience ST relative to the temperature, which is consistent

with magnetic studies. Each metal ion is connected to four other metal ions by 2,4-bpt ligands, giving rise to 2D square-grid sheets, the windows of which are defined by [M(2,4-bpt)] units. Two consecutive layers are organised in a staggered fashion with interlayer π–π stacking interactions (3.4 Å) and C–H···N hydrogen bonds (3.1–3.8 Å), leading to a 3D close-packed structure (Figure 2).

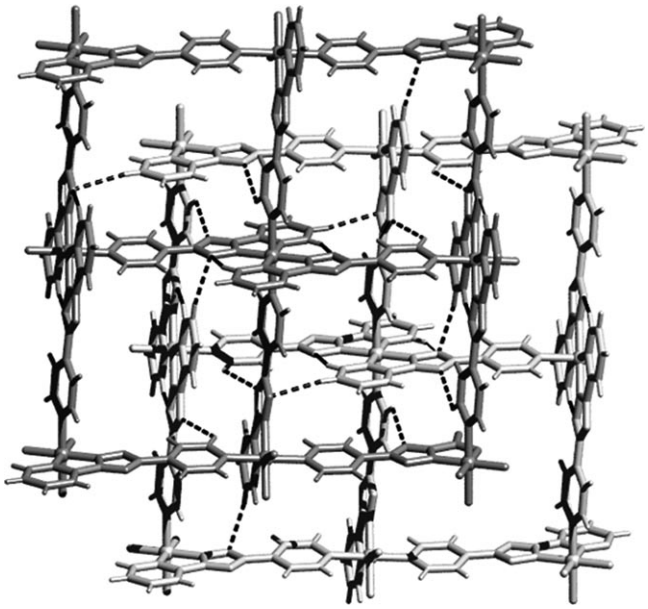

Figure 2. 2D layer structure of **1**·Fe. Dotted lines represent intra- and interlayer hydrogen bonds.

In further structure–magneto studies on **1**·Fe–Co, the temperature dependence of single-crystal X-ray diffraction were carried out over the course of ST. Though the unit-cell parameters do not show regular changes (Figure S7 in the Supporting Information), the variation of average Fe–N bond length shows features similar to that observed in the temperature-dependent magnetic susceptibility studies, namely, abrupt ST with a hysteresis loop in a similar temperature region (Figure 3).

The space groups of **2a**, **2b** and **3** are trigonal $R\bar{3}$, $R\bar{3}c$ and $R\bar{3}$, respectively. Neither space groups nor spin states changed for the three isomers at up to 100 °C (all LS states in three complexes, see $<$Fe–N$>$ in Table S1 in the Supporting Information). All three isomers have similar 3D porous frameworks with NbO topologies. However, compound **3** is non-interpenetrating, whereas **2a** and **2b** are twofold interpenetrating nets through internet C–H···π interactions (about 3.7 Å between closest C atoms). There are hexagonal channels with window diameter dimensions of 5.7, 5.6 and 8.6 Å in **2a**, **2b** and **3**, respectively, along the *c* axes (Figure 4). The vertices and edges are defined by the iron atoms and the 2,4-bpt ligands, respectively. Besides the hexagonal channels seen along the *c* axes, right- and left-handed trigonal channels alternate around the hexagonal voids by sharing 2,4-bpt edges in **2b** and **3**. The channels account for 22.3, 27.1 and 63.5 % of the total crystal volumes of **2a**, **2b** and **3**, respectively, and are filled with guest molecules. Larger guest molecules in **3** can act as templates that stabilise larger voids and avoid interpenetration. The subtle changes in the three isomers can been attributed to the two above-mentioned reasons: 1) the relative orientation of the axial and equatorial ligands; and 2) degrees of two pyridine rings deviating from the plane defined by the triazolate rings, which also affect the direction of Fe···Fe connections.

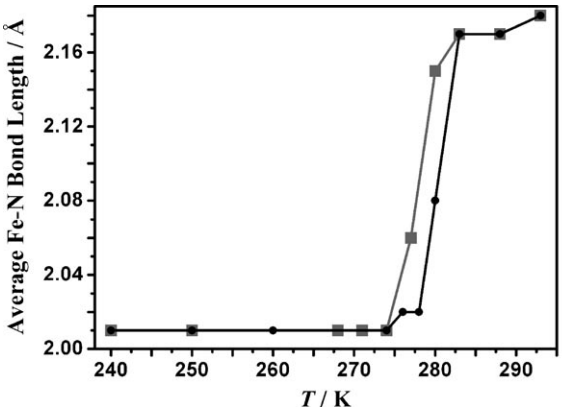

Figure 3. Evolution of the average Fe–N bond length $<$Fe–N$>$ of **1**·Fe–Co from single-crystal X-ray diffraction data over the course of SCO. Data at 283 and 288 K (grey squares) were recorded in a second cooling process after the warming mode.

In our examples, SCO versus non-SCO phenomena in 2D and 3D supramolecular isomers seem to originate from structural architectures rather than guest molecules, as evidenced by crystallographic data at 100 °C for **2a** and **2b**. Firstly, the average Fe–N bond length ($<$Fe–N$>$) gives a reasonable explanation of decrease of ligand field strength in the 2D branch. The temperatures at which single-crystal X-ray measurements were carried out for **1**·Fe are lower than those for the 3D series, but $<$Fe–N$>$ in **1**·Fe is still longer than the other three. As the ligand field strength of 10 Dq is proportional to $1/R$,[14] in which R represents $<$Fe–N$>$, a decrease of 10 Dq around the Fe site of isomer **1**·Fe is clear when compared with the other three. Secondly, in most cases, a hydrogen bond plays an important role in tuning the SCO properties by changing the ligand field strength. But in our case, we would like to compare the hydrogen bond to a spring. In the 3D series, there are three pairs of hydrogen bonds in $[Fe(2,4\text{-bpt})_4]$ building blocks that pull four ligands together and prevent the expansion of the Fe^{II} ion (Figure S9 in the Supporting Information). No other supramolecular interactions, except C–H···π interactions, exist within the framework. In contrast, only one pair of hydrogen bonds exist in $[Fe(2,4\text{-bpt})_4]$ building blocks in the 2D series due to the different relative orientation of axial and equatorial positions, thereby, the pulling force is relatively reduced. Moreover, hydrogen bonds between two adjacent layers have an opposite role, that is, they drag the ligands away from the Fe^{II} centre and prefer HS states. Therefore, in a SCO process, intra- and interlayer hydrogen

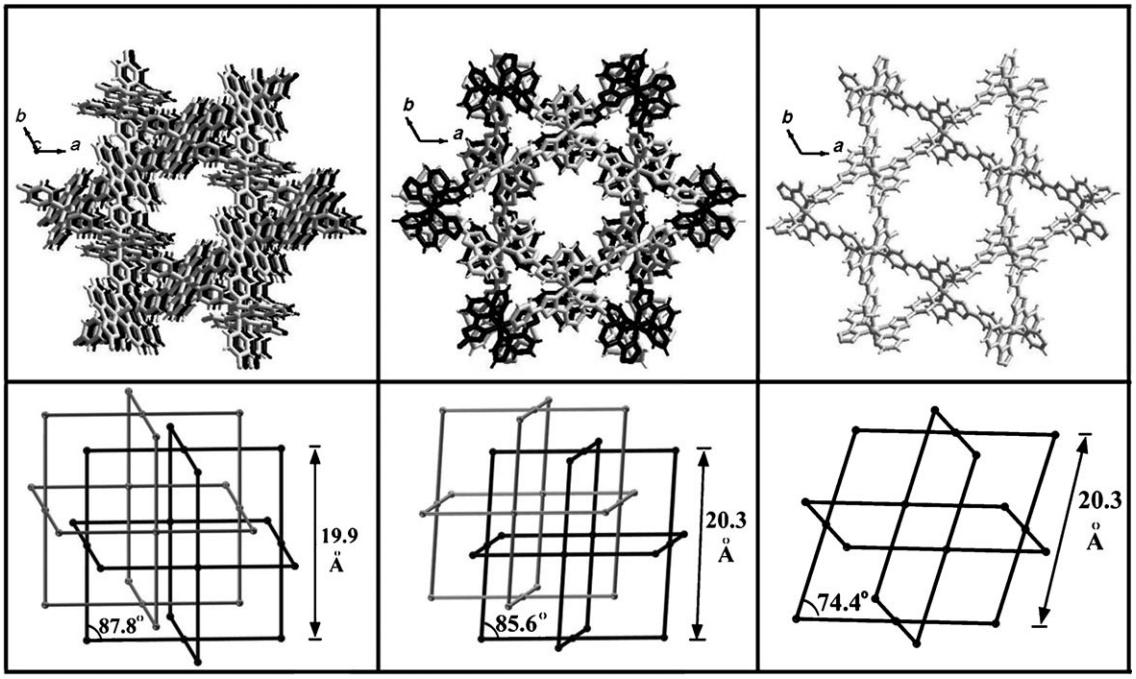

Figure 4. 1D channels propagate along the *c* axes in wires representations (above) and fragments of the NbO nets (below) in **2a** (left), **2b** (middle) and **3** (right), respectively.

bonds compress or expand like springs to balance two spin states. Finally, the absence or existence of π–π stacking interactions in 3D and 2D series, respectively, may also play an important role in magnetic behaviour.

In conclusion, we offer a deep insight into the structural–magneto relationship of four isomers based on the $[Fe(2,4\text{-bpt})_2]$·guest; this includes structural, conformational and catenane supramolecular isomerism. According to their structural and magnetic features, the four isomers can be divided into two categories: 2D SCO and 3D porous LS polymers. Subtle changes in the ligands lead to entirely different structural architectures and magnetic properties through tuning the direction of Fe···Fe connections and supramolecular interactions, respectively. They are 1) the relative orientation of the axial and equatorial ligands; and 2) degrees of two pyridine rings deviating from the plane defined by the triazole ring. Furthermore, by a seed-induced synthetic method, a high yield Fe–Co solid solution was produced and characterised to allow for further studies of magneto–structural relationships. Further systemic research of the Fe–Co solid solution species $[Fe_xCo_{1-x}(2,4\text{-bpt})_2]$ as well as the adsorption behaviour of 3D porous species is in progress.

Experimental Section

General: DSC measurements were carried out on powdered samples of **1**·Fe–Co by using a Netzsch DSC 204 instrument under liquid nitrogen at a scan rate of 5 K min^{-1} in both heating and cooling modes. The Co-to-Fe ratio of **1**·Fe–Co was determined by means of energy-dispersive X-ray spectroscopy (EDXS) (S-520/INCA 300). Magnetic susceptibility measurements were performed on a Quantum Design MPMS-XL7 SQUID instrument, and diamagnetic corrections were made with Pascal's constants. Mössbauer experiments were carried out by using a ^{57}Co/Rh source in a constant-acceleration transmission spectrometer. The spectra were recorded at 20 K in both cooling and heating modes. The spectrometer was calibrated by using a standard α-Fe foil.

Crystal data of 1·Fe at 123(2) K: $C_{24}H_{16}FeN_{10}$; $M_r = 500.32$ g mol^{-1}; monoclinic; space group $P2_1/n$; $a = 8.8598(2)$, $b = 14.4118(4)$, $c = 9.0807(3)$ Å; $\beta = 104.708(3)°$; $V = 1121.48(5)$ Å^3; $Z = 2$; $\rho = 1.482$ g cm^{-3}; $\theta_{max} = 27.50°$; total data 4521; unique data 2532; $\mu = 0.708$ mm^{-1}; 160 parameters; $R_1 = 0.0409$ for $I \geq 2\sigma(I)$ and $wR_2 = 0.0811$ for all data.

Crystal data of 1·Fe at 293(2) K: $a = 8.9558(10)$, $b = 14.7720(17)$, $c = 9.1803(13)$ Å; $\beta = 107.028(4)°$; $V = 1161.3(2)$ Å^3; $Z = 2$; $\rho = 1.431$ g cm^{-3}; $\theta_{max} = 27.50°$; total data 16391; unique data 2652; $\mu = 0.684$ mm^{-1}, 160 parameters; $R_1 = 0.0340$ for $I \geq 2\sigma(I)$ and $wR_2 = 0.0924$ for all data.

Crystal data of 1·Co at 150(2) K: $C_{24}H_{17}CoN_{10}O_{0.5}$; $M_r = 512.41$ g mol^{-1}; monoclinic; space group $P2_1/n$; $a = 9.0044(9)$, $b = 14.7264(13)$, $c = 9.1120(10)$ Å; $\beta = 106.622(12)°$; $V = 1157.8(2)$ Å^3; $Z = 2$; $\rho = 1.470$ g cm^{-3}; $\theta_{max} = 59.99°$; total data 2802; unique data 1632; $\mu = 6.124$ mm^{-1}; 169 parameters; $R_1 = 0.0371$ for $I \geq 2\sigma(I)$ and $wR_2 = 0.0790$ for all data.

Crystal data of 1·Fe-Co at 240(2) K: $C_{24}H_{16}Co_{0.07}Fe_{0.93}N_{10}$; $M_r = 500.53$ g mol^{-1}; monoclinic; space group $P2_1/n$; $a = 8.9225(7)$, $b = 14.3864(11)$, $c = 9.1726(8)$ Å; $\beta = 104.619(3)°$; $V = 1139.30(16)$ Å^3; $Z = 2$; $\rho = 1.459$ g cm^{-3}; $\theta_{max} = 27.00°$; total data 5941; unique data 2260; $\mu = 0.704$ mm^{-1}; 157 parameters; $R_1 = 0.0492$ for $I \geq 2\sigma(I)$ and $wR_2 = 0.1496$ for all data.

Crystal data of 1·Fe-Co at 293(2) K: $a = 9.042(3)$, $b = 14.798(4)$, $c = 9.189(2)$ Å; $\beta = 106.821(8)°$; $V = 1177.0(5)$ Å^3; $Z = 2$; $\rho = 1.431$ g cm^{-3}; $\theta_{max} = 27.48°$; total data 6083; unique data 2415; $\mu = 0.681$ mm^{-1}; 160 parameters; $R_1 = 0.0611$ for $I \geq 2\sigma(I)$ and $wR_2 = 0.1528$ for all data.

Crystal data of 2a at 173(2) K: $C_{24}H_{20.33}FeN_{10}O_{2.17}$; $M_r = 539.35$ g mol^{-1}; trigonal; space group $R\bar{3}$; $a = 27.608(4)$, $c = 8.937(3)$ Å; $V = 5899(2)$ Å^3; $Z = 9$; $\rho = 1.366$ g cm^{-3}; $\theta_{max} = 26.24°$; total data 9293; unique data 2581; $\mu = 0.617$ mm^{-1}; 169 parameters; $R_1 = 0.0799$ for $I \geq 2\sigma(I)$ and $wR_2 = 0.2576$ for all data.

Crystal data of 2a at 293(2) K: $a = 27.787(4)$, $c = 9.1222(14)$ Å; $V = 6099.8(16)$ Å^3; $Z = 9$; $\rho = 1.321$ g cm^{-3}; $\theta_{max} = 27.46°$; total data 11623;

unique data 3078; $\mu = 0.597\ mm^{-1}$; 161 parameters; $R_1 = 0.0642$ for $I \geq 2\sigma(I)$ and $wR_2 = 0.2316$ for all data.

Crystal data of 2a at 373(2) K: $C_{24}H_{16}FeN_{10}$; $M = 500.32\ g\,mol^{-1}$; $a = 27.8061(17)$, $c = 9.0879(9)$ Å; $V = 6085.2(8)$ Å^3; $Z = 9$; $\rho = 1.229\ g\,cm^{-3}$; $\theta_{max} = 27.00°$; total data 5751; unique data 2810; $\mu = 0.587\ mm^{-1}$; 160 parameters; $R_1 = 0.0748$ for $I \geq 2\sigma(I)$ and $wR_2 = 0.2641$ for all data.

Crystal data of 2b at 293(2) K: $C_{24}H_{22}FeN_{10}O_3$; $M_r = 554.37\ g\,mol^{-1}$; trigonal; space group $R\bar{3}c$; $a = 29.710(6)$; $c = 16.145(7)$ Å; $V = 12342(6)$ Å^3; $Z = 18$; $\rho = 1.343\ g\,cm^{-3}$; $\theta_{max} = 26.99°$; total data 9800; unique data 2802; $\mu = 0.594\ mm^{-1}$; 173 parameters; $R_1 = 0.0780$ for $I \geq 2\sigma(I)$ and $wR_2 = 0.2334$ for all data.

Crystal data of 2b at 373(2) K: $C_{24}H_{16}FeN_{10}$; $M_r = 500.32\ g\,mol^{-1}$; $a = 29.932(6)$, $c = 16.139(4)$ Å; $V = 12522(5)$ Å^3; $Z = 18$; $\rho = 1.194\ g\,cm^{-3}$; $\theta_{max} = 26.99°$; total data 9600; unique data 2983; $\mu = 0.571\ mm^{-1}$; 161 parameters; $R_1 = 0.0850$ for $I \geq 2\sigma(I)$ and $wR_2 = 0.2497$ for all data.

Crystal data of 3 at 150(2) K: $C_{40}H_{56}FeN_{10}O_{12}$; $M_r = 924.80\ g\,mol^{-1}$; trigonal; space group $R\bar{3}$; $a = 32.1469(10)$, $c = 11.8998(7)$ Å; $V = 10650.0(8)$ Å^3; $Z = 9$; $\rho = 1.298\ g\,cm^{-3}$; $\theta_{max} = 26.98°$; total data 15996; unique data 5005; $\mu = 0.386\ mm^{-1}$; 287 parameters; $R_1 = 0.0811$ for $I \geq 2\sigma(I)$ and $wR_2 = 0.2898$ for all data.

Crystal data of 3 at 293(2) K: The solvent molecules were disordered and could not be modelled properly; thus, program SQUEEZE,[15] a part of the PLATON package of crystallographic software, was used to calculate the solvent disorder area and remove its contribution to the overall intensity data. $a = 31.931(2)$, $c = 12.3983(13)$ Å; $V = 10947.6(16)$ Å^3; $Z = 18$; $\rho = 1.710\ g\,cm^{-3}$; $\theta_{max} = 59.98°$; total data 6116; unique data 3550; $\mu = 5.596\ mm^{-1}$; 160 parameters; $R_1 = 0.0480$ for $I \geq 2\sigma(I)$ and $wR_2 = 0.1372$ for all data.

The intensity data of **1**·Co and **3** (293 K) were recorded on an Oxford Diffraction Gemini R CCD diffractometer with $Cu_{K\alpha}$ radiation ($\lambda = 1.54178$ Å). The intensity data of **2b** (293 K) and **2b** (373 K) were recorded on an Oxford Diffraction Gemini R CCD diffractometer with $Mo_{K\alpha}$ ($\lambda = 0.71073$ Å) and on a Bruker SMART Apex CCD system with $Mo_{K\alpha}$ ($\lambda = 0.71073$ Å, respectively. The remaining ones were recorded on a Rigaku R-AXIS SPIDER IP diffractometer with $Mo_{K\alpha}$ ($\lambda = 0.71073$ Å). The structure was solved by direct methods and refined on F^2 by using SHELXTL. CCDC-768301, 768302, 768303, 768304, 768305, 768306, 768307, 768308, 768309, 768310, 768311, and 768312 contain the supplementary crystallographic data for this paper. These data can be obtained free of charge from The Cambridge Crystallographic Data Centre via www.ccdc.cam.ac.uk/data_request/cif.

Acknowledgements

This work was supported by the NSFC (grant no. 20525102, 20821001, 90922009, 50872157 and J0730420) and the 973 Project (2007CB815305).

Keywords: iron · niobium · spin crossover · structural–magneto correlations · supramolecular chemistry

[1] a) O. Kahn, C. Jay Martinez, *Science* **1998**, *279*, 44–48; b) P. Gütlich, H. A. Goodwin, *Top. Curr. Chem.* **2004**, *233*, 1–9; c) O. Kahn, *Molecular Magnetism*, VCH, Weinheim, **1993**, pp. 53–84; d) J.-F. Létard, P. Guionneau, L. Goux-Capes, *Top. Curr. Chem.* **2004**, *235*, 221–249; e) A. Galet, A. B. Gaspar, M. C. Muñz, G. V. Bukin, G. Levchenko, J. A. Real, *Adv. Mater.* **2005**, *17*, 2949–2953; f) M. Cavallini, I. Bergenti, S. Milita, G. Ruani, I. Salitros, Z.-R. Qu, R. Chandrasekar, M. Ruben, *Angew. Chem.* **2008**, *120*, 8724–8728; *Angew. Chem. Int. Ed.* **2008**, *47*, 8596–8600; g) P. Gamez, J. S. Costa, M. Quesada, G. Aromí, *Dalton Trans.* **2009**, 7845–7853.

[2] a) S. Bonhommeau, G. Molnár, A. Galet, A. Zwick, J.-A. Real, J. J. McGarvey, A. Bousseksou, *Angew. Chem.* **2005**, *117*, 4137–4141; *Angew. Chem. Int. Ed.* **2005**, *44*, 4069–4073; b) A. Bousseksou, N. Negre, M. Goiran, L. Salmon, J.-P. Tuchagues, M.-L. Boillot, K. Boukheddaden, F. Varret, *Eur. Phys. J. B* **2000**, *13*, 451–456; c) A. Bousseksou, G. Molnár, G. Matouzenko, *Eur. J. Inorg. Chem.* **2004**, 4353–4369; d) T. Mahfoud, G. Molnár, S. Bonhommeau, S. Cobo, L. Salmon, P. Demont, H. Tokoro, S.-I. Ohkoshi, K. Boukheddaden, A. Bousseksou, *J. Am. Chem. Soc.* **2009**, *131*, 15049–15054.

[3] a) K. S. Murray, *Eur. J. Inorg. Chem.* **2008**, 3101–3121; b) B. Weber, *Coord. Chem. Rev.* **2009**, *253*, 2432–2449; c) J. A. Real, A. B. Gaspar, V. Niel, M. C. Muñoz, *Coord. Chem. Rev.* **2003**, *236*, 121–141; d) J. A. Real, A. B. Gaspar, V. Niel, M. C. Muñoz, *Dalton Trans.* **2005**, 2062–2079; e) P. Gütlich, Y. Garcia, H. A. Goodwin, *Chem. Soc. Rev.* **2000**, *29*, 419–427.

[4] a) M. Ohba, K. Yoneda, G. Agustí, M. C. Muñoz, B. Gaspar, J. A. Real, M. Yamasaki, H. Ando, Y. Nakao, S. Sakaki, S. Kitagawa, *Angew. Chem.* **2009**, *121*, 4861; *Angew. Chem. Int. Ed.* **2009**, *48*, 4767; b) S. M. Neville, B, Moubaraki, K. S. Murray, C. J. Kepert, *Angew. Chem.* **2007**, *119*, 2105–2108; *Angew. Chem. Int. Ed.* **2007**, *46*, 2059–2062; c) P. D. Southon, L. Liu, E. A. Fellows, D. J. Price, G. J. Halder, K. W. Chapman, B. Moubaraki, K. S. Murray, J.-F. Létard, C. J. Kepert, *J. Am. Chem. Soc.* **2009**, *131*, 10998–11009; d) S. M. Neville, G. J. Halder, K. W. Chapman, M. B. Duriska, B. Moubaraki, K. S. Murray, C. J. Kepert, *J. Am. Chem. Soc.* **2009**, *131*, 12106–12108; e) S. M. Neville, G. J. Halder, K. W. Chapman, M. B. Duriska, P. D. Southon, J. D. Cashion, J.-F. Létard, B. Moubaraki, K. S. Murray, C. J. Kepert, *J. Am. Chem. Soc.* **2008**, *130*, 2869–2876; f) M. Seredyuk, A. B. Gaspar, V. Ksenofontov, M. Verdaguer, F. Villain, P. Gütlich, *Inorg. Chem.* **2009**, *48*, 6130–6141; g) M. Bartel, A. Absmeier, G. N. L. Jameson, F. Werner, K. Kato, M. Takata, R. Boca, M. Hasegawa, K. Mereiter, A. Caneschi, W. Linert, *Inorg. Chem.* **2007**, *46*, 4220–4229; h) M. Nihei, L. Han, H. Oshio, *J. Am. Chem. Soc.* **2007**, *129*, 5312–5313; i) A. Galet, M. C. Muñoz, J. A. Real, *Chem. Commun.* **2006**, 4321–4323; j) V. Niel, A. L. Thompson, M. C. Muñoz, A. Galet, A. E. Goeta, J. A. Real, *Angew. Chem.* **2003**, *115*, 3890; *Angew. Chem. Int. Ed.* **2003**, *42*, 3760; k) G. J. Halder, K. W. Chapman, S. M. Neville, B. Moubaraki, K. S. Murray, J.-F. Létard, C. J. Kepert, *J. Am. Chem. Soc.* **2008**, *130*, 17552–17562.

[5] a) M. Yamada, M. Ooidemizu, Y. Ikuta, S. Osa, N. Matsumoto, S. Iijima, M. Kojima, F. Dahan, J.-P. Tuchagues, *Inorg. Chem.* **2003**, *42*, 8406–8416; b) M. Seredyuk, A. B. Gaspar, M. C. Muñoz, M. Verdaguer, F. Villain, P. Gütlich, *Eur. J. Inorg. Chem.* **2007**, 4481–4491; c) D. Chernyshov, M. Hostettler, K. W. Törnroos, H.-B. Bürgi, *Angew. Chem.* **2003**, *115*, 3955–3960; *Angew. Chem. Int. Ed.* **2003**, *42*, 3825–3830; d) B. Weber, E. Kaps, J. Weigand, C. Carbonera, J.-F. Létard, K. Achterhold, F. G. Parak, *Inorg. Chem.* **2008**, *47*, 487–496; e) J. A. Kitchen, N. G. White, M. Boyd, B. Moubaraki, K. S. Murray, P. D. W. Boyd, S. Brooker, *Inorg. Chem.* **2009**, *48*, 6670–6679; f) C. Rajadurai, Z, Qu, O. Fuhr, B. Gopalan, R. Kruk, M. Ghafari, M. Ruben, *Dalton Trans.* **2007**, 3531–3537; g) M. Yamada, H. Hagiwara, H. Torigoe, N. Matsumoto, M. Kojima, F. Dahan, J.-P. Tuchagues, N. Re, S. Iijima, *Chem. Eur. J.* **2006**, *12*, 4536–4549.

[6] a) G. S. Matouzenko, A. Bousseksou, S, Lecocq, P. J. van Koningsbruggen, M. Perrin, O. Kahn, A. Collet, *Inorg. Chem.* **1997**, *36*, 5869–5879; b) S. M. Neville, B. A. Leita, D. A. Offermann, M. B. Duriska, B. Moubaraki, K. W. Chapman, G. J. Halder, K. S. Murray, *Eur. J. Inorg. Chem.* **2007**, 1073–1085; c) D. L. Reger, J. R. Gardiniер, M. D. Smith, A. M. Shahin, G. J. Long, L. Rebbouh, F. Grandjean, *Inorg. Chem.* **2005**, *44*, 1852–1866; d) A. L. Thompson, A. E. Goeta, J. A. Real, A. Galet, M. C. Muñoz, *Chem. Commun.* **2004**, 1390–1391; e) A. Ozarowski, B. R. McGarvey, A. B. Sarkar, J. E. Drake, *Inorg. Chem.* **1988**, *27*, 628–635; f) A. Galet, A. B. Gaspar, M. C. Munñoz, G. Levchenko, J. A. Real, *Inorg. Chem.* **2006**, *45*, 9670–9679; g) V. Ksenofontov, A. B. Gaspar, G. Levchenko, B. Fitzsimmons, P. Gu1tlich, *J. Phys. Chem. B* **2004**, *108*, 7723–7727; h) C.-F. Sheu, S.-M. Chen, S.-C. Wang, G.-H. Lee, Y.-H. Liu, Y. Wang, *Chem. Commun.* **2009**, 7512–7514; i) C.-F. Sheu, K. Chen, S.-M. Chen, Y.-S. Wen, G.-H. Le, J.-M. Chen, J.-F. Lee, B.-M. Cheng, H.-S. Sheu, N. Yasuda, Y. Ozawa, K. Toriumi, Y. Wang, *Chem. Eur. J.* **2009**, *15*, 2384–2388; j) R. Pritchard, H. Lazar, S. A. Barrett,

C. A. Kilner, S. Asthana, C. Carbonera, J.-F. Létard, M. A. Halcrow, *Dalton Trans.* **2009**, 6656–6666; k) M. Haryono, F. W. Heinemann, K. Petukhov, K. Gieb, P. Müller, A, Grohmann, *Eur. J. Inorg. Chem.* **2009**, 2136–2143; l) C.-F. Sheu, S. Pillet, Y. C. Lin, S. M. Chen, I.-J. Hus, C. Lecomte, Y. Wang, *Inorg. Chem.* **2008**, *47*, 10866–10874; m) G. Agustí, C. Bartual, V. Martínez, F. J. Muñoz-Lara, A. B. Gaspar, M. C. Muñoz, J. A. Real, *New J. Chem.* **2009**, *33*, 1262–1267.

[7] a) A. Galet, M. C. Muñoz, A. B. Gaspar, J. A. Real, *Inorg. Chem.* **2005**, *44*, 8749–8755; b) A. Galet, M. C. Muñoz, V. Martínez, J. A. Real, *Chem. Commun.* **2004**, 2268–2269; c) G. Agustí, M. C. Muñoz, A. B. Gaspar, J. A. Real, *Inorg. Chem.* **2009**, *48*, 3371–3381.

[8] a) B. Moulton, M. J. Zaworotko, *Chem. Rev.* **2001**, *101*, 1629–1658; b) M.-L. Tong, S. Hu, J. Wang, S. Kitagawa, S. W. Ng, *Cryst. Growth Des.* **2005**, *5*, 837–839.

[9] a) M. H. Klingele, S. Brooker, *Coord. Chem. Rev.* **2003**, *241*, 119–132; b) J. A. Kitchen, S. Brooker, *Coord. Chem. Rev.* **2008**, *252*, 2072–2092; c) M.-X. Peng, C.-G. Hong, C.-K. Tan, J.-C. Chen, M.-L. Tong, *J. Chem. Crystallogr.* **2006**, *36*, 703–707; d) J.-C. Chen, S. Hu, A.-J. Zhou, M.-L. Tong, Y.-X. Tong, *Z. Anorg. Allg. Chem.* **2006**, *632*, 475–481; e) M.-L. Tong, C.-G. Hong, L.-L. Zheng, M.-X. Peng, A. Gaita-Ariño, J. M. Clemente Juan, *Eur. J. Inorg. Chem.* **2007**, 3710–3717; f) Z.-S. Meng, L. Yun, W.-X. Zhang, C.-G. Hong, R. Herchel, Y.-C. Ou, J.-D. Leng, M.-X. Peng, Z. Lin, M.-L. Tong, *Dalton Trans.* **2009**, 10284–10295; g) X. Bao, J.-D. Leng, Z.-S. Meng, Z.-J. Lin, M.-L. Tong, M. Nihei, H. Oshio, *Chem. Eur. J.* **2010**, *16*, 6169–6174.

[10] These two mononuclear complexes will be reported in a subsequent full paper.

[11] a) T. Ezuhara, K. Endo, Y. Aoyama, *J. Am. Chem. Soc.* **1999**, *121*, 3279–3283; b) D. Braga, F. Grepioni, *Angew. Chem.* **2004**, *116*, 4092–4102; *Angew. Chem. Int. Ed.* **2004**, *43*, 4002–4011; c) D. Braga, F. Grepioni, *Chem. Commun.* **2005**, 3635–3645.

[12] a) M. Sorai, J. Ensling, P. Gütlich, *Chem. Phys.* **1976**, *18*, 199–205; b) A. Hauser, P. Gütlich, H. Spiering, *Inorg. Chem.* **1986**, *25*, 4245–4248; c) A. Hauser, *Coord. Chem. Rev.* **1991**, *111*, 275–290; d) I. Sanner, E. Meissner, H. Köppen, H. Spiering, P. Gütlich, *Chem. Phys.* **1984**, *86*, 227–233; e) C. A. Tovee, C. A. Kilner, J. A. Thomas, M. A. Halcrow, *CrystEngComm* **2009**, *11*, 2069–2077.

[13] J.-B. Lin, J.-P. Zhang, W.-X. Zhang, W. Xue, D.-X. Xue, X.-M. Chen, *Inorg. Chem.* **2009**, *48*, 6652–6660.

[14] T. Tayagaki, A. Galet, G Molnár, M. C. Munõz, A. Zwick, K. Tanaka, J. A. Real, A. Bousseksou, *J. Phys. Chem. B* **2005**, *109*, 14859–14867.

[15] P. van der Sluis, A. L. Spek, *Acta Crystallogr. Sect. A* **1990**, *46*, 194–201.

Received: May 3, 2010
Published online: June 10, 2010

